Simulation of 3D-Silicon sensor with a Low-Gain Avalanche Diode (LGAD) for a fast timing pixel detector

I. ABSTRACT

Presently, the silicon pixel detector either has no proper timing or has proper timing, but with a pixel size at the mm level, too large for precision tracking. The 3D-sensor has excellent spatial resolution and it could potentially be a fast timing detector with a timing resolution of ≈30 ps as demonstrated by the recent study. In this study, we present some preliminary results on the 3D-LGAD sensor based TCAD simulation, which could improve the signal-to-noise ratio to achieve a better timing resolution. We aim to develop a truly 4-D silicon pixel detector with 3D sensor with both a spatial resolution of ≈ 10 μm and a timing resolution of ≈30 ps that will open a new era for precision tracking, reducing pile-up events and particle identification for the future colliding experiment.

II. INTRODUCTION

Silicon detectors provide at present the most precise tracking for charged particles in high energy physics experiments. They have an excellent space point resolution and granularity to cope track separation in dense jets and hits from the high luminosity beam related background. The recent developments of a new silicon sensor based on Low-Gain Avalanche Diodes (LGAD) provide a significantly enhanced capability to measure track arrival times with a resolution of ≈30 ps, which allows for tracks to be separated from pile-up events and particle identification. Presently, the silicon pixel detector either has no proper timing or has proper timing, but with a pixel size at the mm level, too large for precision tracking.

The 3D sensor was first introduced in 1997 by S. Parker et al. [**?**]. It decouples the electrode distance from the active substrate thickness providing several superior features, which makes it more radiation hard, and fast charge collection compared to the planar sensor. The first application of 3D sensors was successfully installed for the ATLAS Insertable B-Layer (IBL), and the sensor design has been further improved for the HL-LHC developed by CNM [**?**] and FBK [**?**]. The recent study with a small cell 3D sensor demonstrated that it could potentially be a fast timing detector with a resolution of ≈30 ps [**?**].

The idea proposed here is to develop a new type of 3D sensor with internal charge multiplication by adding a thin low-resistivity diffusion gain layer surrounding the readout electrode with a highly doped implant. The thin layer will enhance the high electric field to cause multiplication of charge carries that transverse the region, which will improve the signal-to-noise ratio to achieve a timing resolution better than ≈30 ps. From a simple calculation, the gain is similar to what obtained in the planar LGAD detector.

III. LGAD

The planar LGAD detector has a gain layer that contains high electric field to cause multiplication of charge carries that transverse the region. The gain is achieved by raising the electric field high enough to enable the charge carriers to create secondary ionization during the charge collection process. The main difference to standard APD detectors are the low gain required to detect high energy charged particles in the thin sensors. With the low gain these sensors can be very thin to have a fast drift time and have enough signal-to-noise ratio to achieve good time resolution.

The fast timing detector has been studied extensively for HL-LHC upgrades where the excellent time resolution coupled with good spatial resolution can help to reduce pile-up events. ATLAS has recently proposed to use the High Granularity Timing Detector (HGTD) in the forward region and CMS is considering adding a timing layer in the barrel region with SIPM for photon detection, while using HGTD in the forward region. In both cases, the timing detector is limited to have a pad size of 1 mm x 1 mm with a time resolution of ≈30 ps, but this size is too large to be useful for precision tracking.

The timing resolution is determined mainly by contributions from time walk and noise jitter. The time walk contribution is usually minimized by using Constant Fraction Discrimination (CFD) or determining time of the signal crossing fixed threshold. The jitter contribution is determined by the rise of the signal at the output of the amplifier and noise level. The timing resolution can be improved with larger gain as well as with thin detectors since both increase the slew-rate of the amplifiers. However, the time walk is dominated by Landau fluctuations due to the non-uniform charge deposition within the sensors, especially for LGADs where electrons need to reach the gain layer to multiply

IV. TCAD SIMULATION

The simulation is performed using the Synopsys Sentaurus TCAD simulation toolkit to understand the elctrical behavior for the proposed 3D-LGAD sensor. We use the same TCAD setup for the ATLAS IBL 3D pixel detector study and simply add an extra thin low-resistivity p+ doping gain layer of 3 μ thick surrounding the n+ readout electrode. The IBL 3D pixel cell consists of two connected n+ readout electrodes (2E) surrounded by eight p+ electrodes with a size of 50x250x230 μm^3 as shown in Fig. 1. We use a reduced red rectangle area in TCAD simulation to save time by taking the advantage of 8-fold symmetry of IBL 3D pixel.

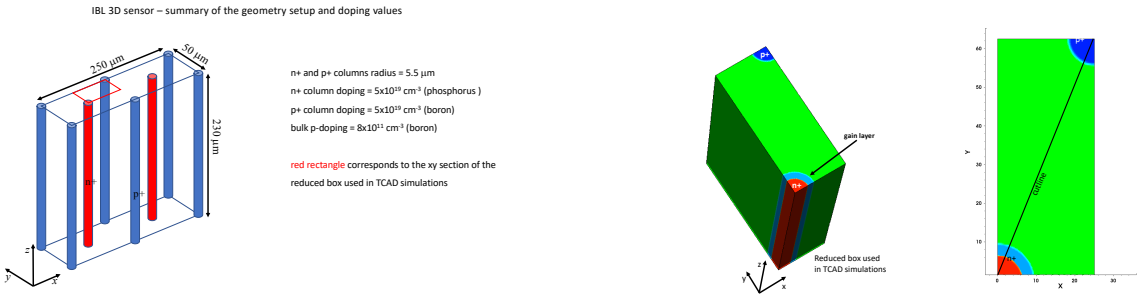

FIG. 1: A schematic view of IBL 3D pixel sensor (right) and the reduced box used in TCAD simulation (right).

A. Electric properties

We have considered different values for the p+ doping concentration of the gain layer (ranging from 10^{14} to 10^{16} cm^{-3}). For higher gain layer doping concentrations, breakdown takes place before the depletion. Fig. 2 shows the electric field maps and projection along the diagonal line between n+ and p+ electrodes with a bias voltage of 100 V for the unirradiated sensor. The results for irradiated sensor at fluence of 1.0e 15 neq/cm^2 are also studied and they do not display any significant change. As the gain layer doping is increased, the electric field shows expected increase in the gain layer region.

The current-voltage (I-V) curves and the capacitance-voltage ($1/C^2$-V) curves are also checked for different doping densities of the gain layer (GL) as shown in Fig. 3 with non-irradiated sensor. There is a prefect correspondence between the jumps in the I-V curves and the jumps in $1/C^2$ - V curves, which should be a clear signature of depletion. Note that the current values are so small because they correspond to the current for only the reduced box used for the TCAD simulation; for comparison to a practical measure they should be rescaled by taking into account the number of the sensors in a module.

B. Charge collection and timing resolution

A Minimum Ionizing Particle (MIP) is simulated for charge collection using the TCAD simulation. Fig. 4 shows the sketch of the reduced sensor area with different positions marked for the MIP passing through perpendicularly. The simulation is done only for a 1 μm thick slice for saving time since the electric field does not change much with sensor thickness and we expect the results obtained here should be rather consistent with those one would obtain with larger sensor thickness.

Fig. 5-9 show the current and collected charge at the readout electrode for hits at points of A, C, E, G, and I, at different bias voltages of 60, 100, and 200 V, and for increasing the GL doping values. The same scale is used in all graphs, which allows to clearly appreciate the increase in current and collected charge as the GL doping reach high values. A deposited charge by MIP of 80 e (electron charge) per um were considered and collected charge is expressed as charge fraction with respect to the deposited one. In our case, since the sensor thickness is 1 um, a charge fraction

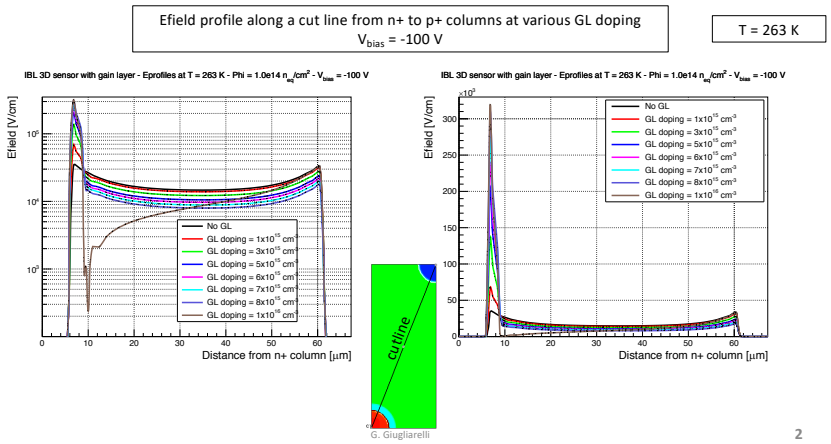

FIG. 2: The projection of the electric field along the diagonal line between n+ and p+ electrodes with a bias voltage of 100V in a log-scale (left) and a linear-scale (right).

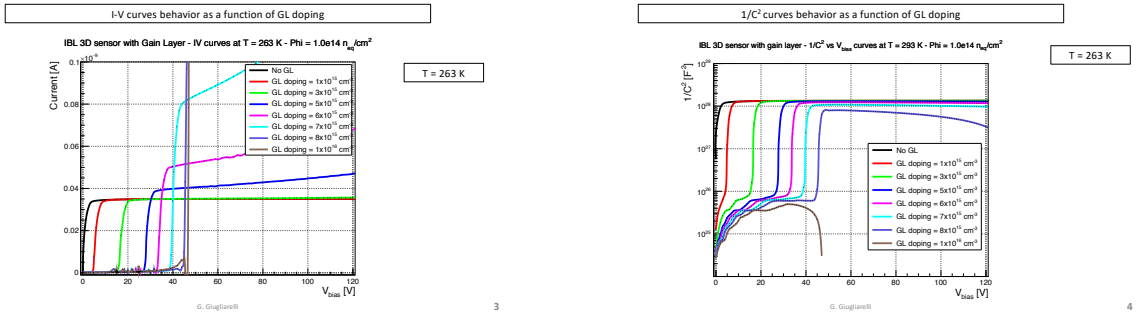

FIG. 3: The curves for I-V (left) and $1/C^2$-V (right) are shown for the GL with different doping densities.

of 1 means a collected charge = 80 e. Note how collected charge for GL doping near 7x10^{1}5 cm$^-$3 becomes, because of avalanches, also larger than 5 times the deposited charge.

The timing of arrival at 50% of charge pulse height resolution (TOA50) is measured for these hits as a function of the distance from the n+ readout electrode in the transverse plane for different bias voltages and the GL doping densities. The results are summarized in Fig. 10, which seems intuitive that the central hits have the lowest TOA. Fig. 11 shows the average mean of TOA50 and its RMS from 9 hit points as a function of the GL doping density for different bias voltage, respectively. The trend seems clear that the increase of TOA50 going from no GL to a higher GL doping density, which is caused by the slow drift of holes produced from the avalanches. However, more studies are need to understand better the avalanche process in TCAD simulation and the noise level of the front end electronics.

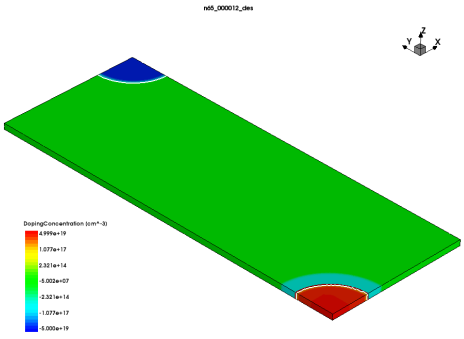

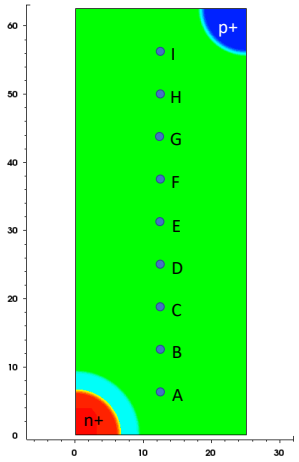

Charge collection for MIPs where obtained for a 1 µm thick slice. Perpendicular hits where considered at the 9 points (A, B, …., I) marked in the rigth picture.

G. Giugliarelli 5

FIG. 4: The sketch of the reduced sensor area with different positions marked for the MIP passing through perpendicularly in TCAD simulation.

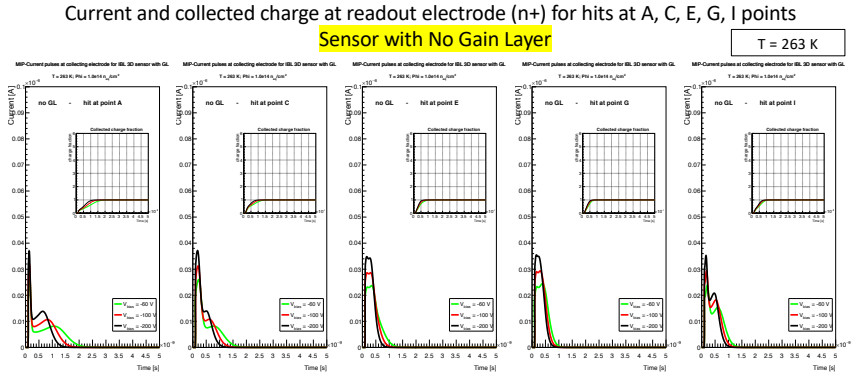

G. Giugliarelli 6

FIG. 5: The currents and collected charges as a function of time are shown for different hit positions and bias voltages with no GL 3D sensor.

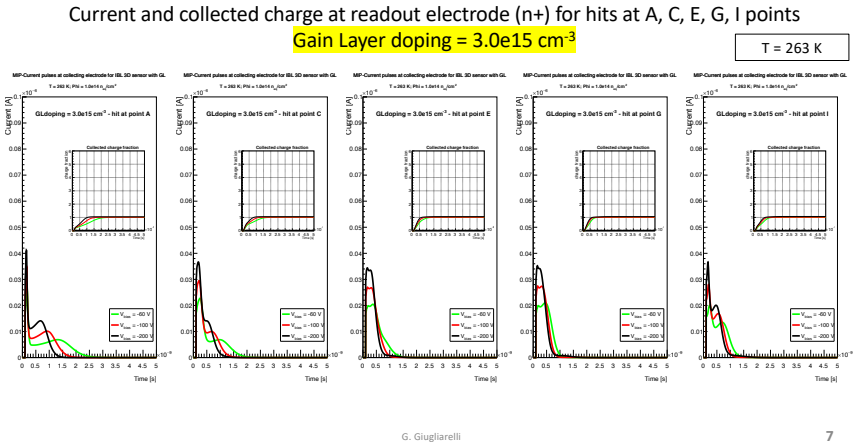

FIG. 6: The currents and collected charges as a function of time are shown for different hit positions and bias voltages with a GL doping density of $3x10^{15}$ cm^{-3}.

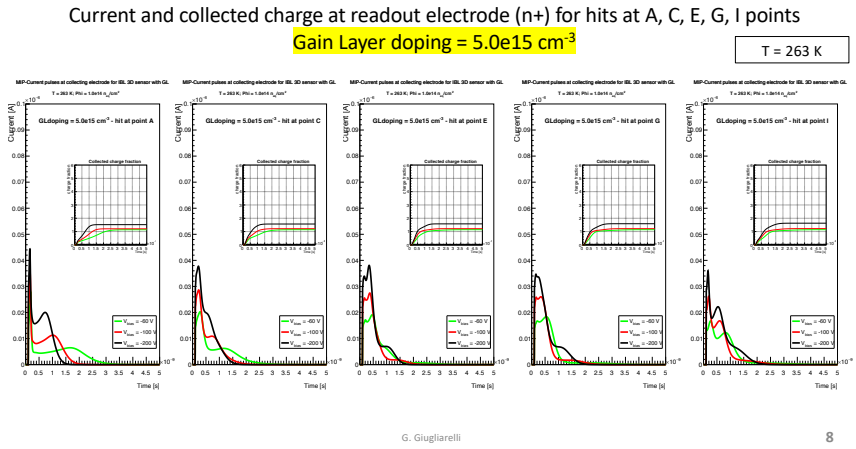

FIG. 7: The currents and collected charges as a function of time are shown for different hit positions and bias voltages with a GL doping density of $5x10^{15}$ cm^{-3}.

V. ALTERNATIVE STUDIES WITH KDETSIM

We also performed the studies using KDetSim [**?**] to simulate the charge collection in the proposed 3D-GLAD sensor. The charge drift is simulated in steps with diffusion, impact ionization, and trapping also taken into account and the induced current is then proceeded with a transfer function of a front-end electronics with a shaping time of 1 ns. The results obtained from KDetSim are consistent with TCAD simulation. Fig. 12 shows the projected electric

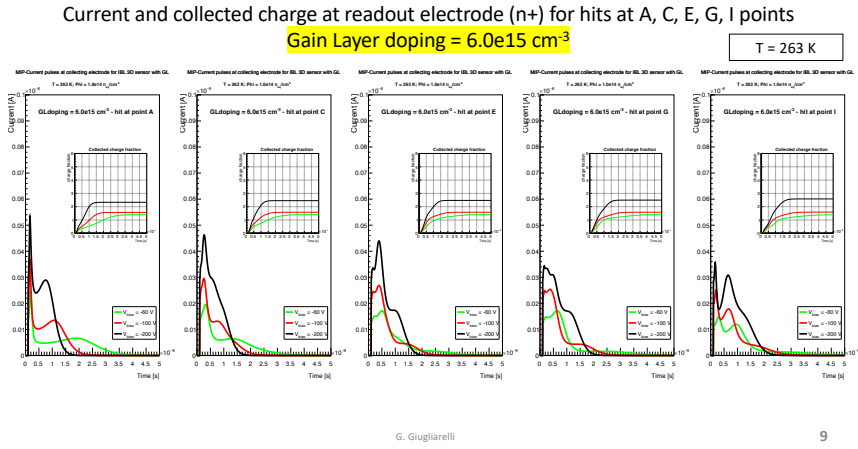

FIG. 8: The currents and collected charges as a function of time are shown for different hit positions and bias voltages with a GL doping density of $6x10^{15}$ cm^{-3}.

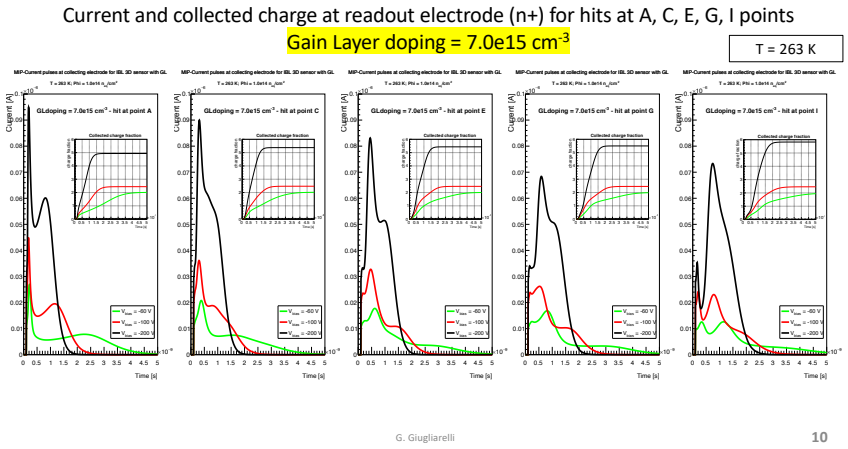

FIG. 9: The currents and collected charges as a function of time are shown for different hit positions and bias voltages with a GL doping density of $7x10^{15}$ cm^{-3}.

fields (V/um) and the average charge collection gains for a MIP passing through randomly and perpendicularly to the detector as a function of GL doping densities and the bias voltage. Fig. 13 shows the drift-time (TOA50) as a function of drift distance from the n+ electrode as well as the average TOA50 before and after the drift-time corrections based on the drift distance. The average TOA50 seems increased for a higher doping density GL, which is mainly due to increased the number of holes from the impact ionization process. However, after the drift-distance correction, the TOA50 timing resolution can be greatly improved to below 30 ps.

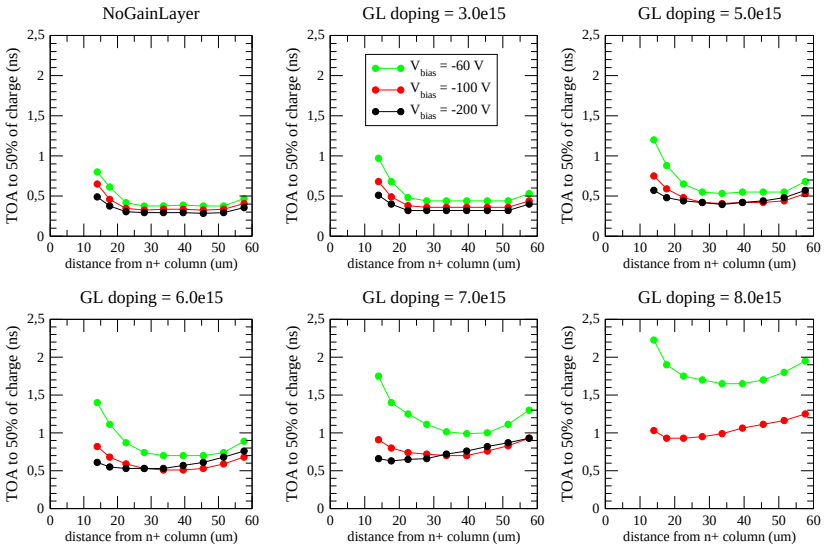

FIG. 10: The measured TOA50 as a function of the distance between the hit position and the readout electrode in the transverse plane for different bias voltages and the GL doping densities.

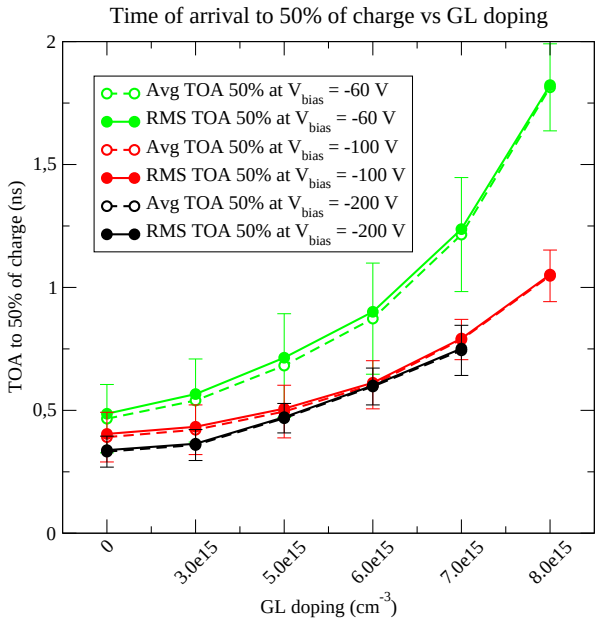

FIG. 11: The averages and RMS of 9 measured TOA50 as a function of GL densities and with different bias voltages.

VI. CHALLENGS

The 3D-LGAD sensor could be difficult to produce in large-scale due to the challenges of properly doping the electrodes. The electrodes are normally made by depositing the poly-silicon inside the holes and they are doped by diffusion from solid or liquid source. An alternative procedure is required to dope the gain layer properly.

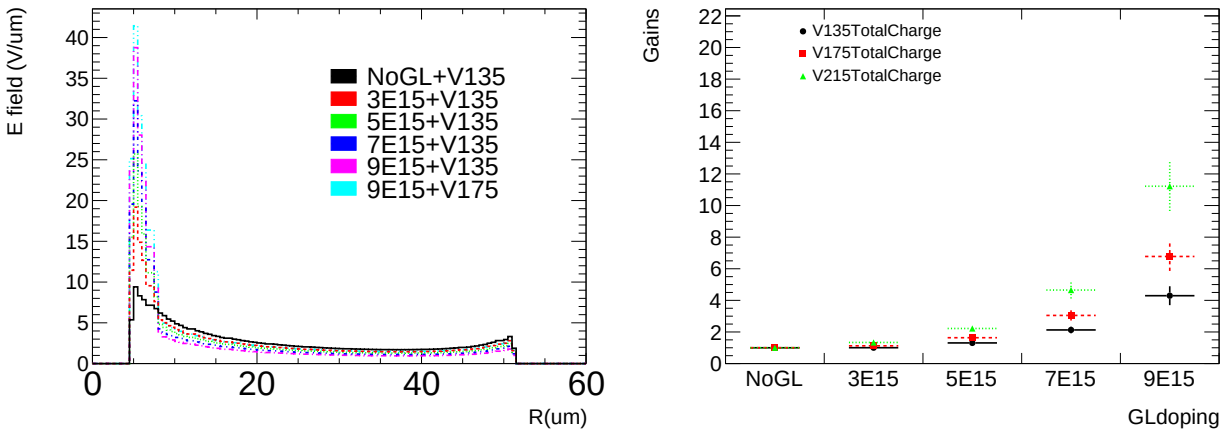

FIG. 12: The projection of the electric fields along the diagonal line between n+ and p+ electrodes (left) and the average charge collection gains for a MIP (right) as a function of GL doping densities and the bias voltages.

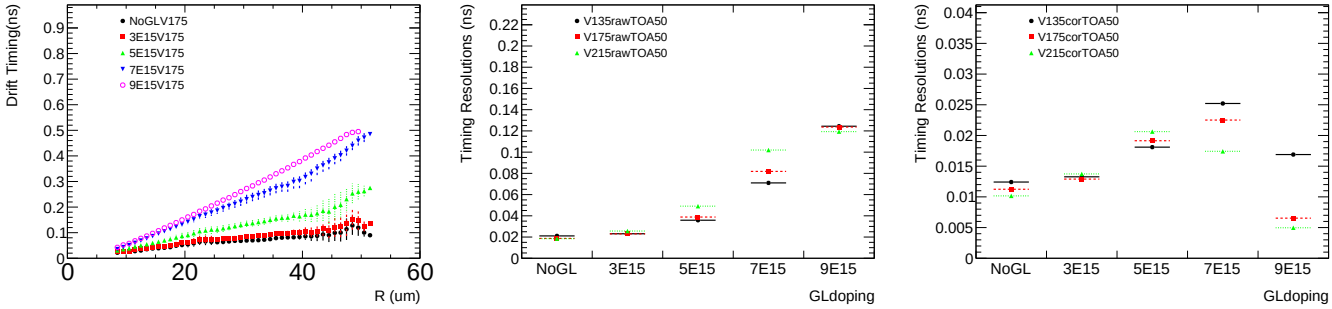

FIG. 13: The drift-time (TOA50) as a function of drift distance from the n+ electrode (left); the average TOA50 before (middle) and after (right) the drift-time corrections.

There are also significant challenges to develop the next generation of readout ASIC chips with a pixel size of 50x50 μm^2 and a timing resolution of $\approx$ 30 ps. The current RD53 chip has a correct pixel size, but it has no proper timing resolution. On the other hand, the ALTIROC chip designed for HGTD at ATLAS has a timing resolution of 20 ps, but its pixel size is 1.3 mm x 1.3 mm, too large for precision tracking [**?**].

VII. CONCLUSION

In this study, we present some preliminary results on the 3D-LGAD sensor based TCAD simulation, which could improve the signal-to-noise ratio to achieve a better timing resolution. We aim to develop a truly 4-D silicon pixel detector with 3D sensor with both a spatial resolution of $\approx$ 10 μm and a timing resolution of $\approx$30 ps that will open a new era for precision tracking, reducing pile-up events and particle identification for the future colliding experiment.

[1] S. I. Parker, et al., 3-D: A New architecture for solid state radiation detectors, Nucl. Instrum. Meth. A395 (1997) 328–343.
[2] G. Pellegrini, et al., First double-sided 3-D detectors fabricated at CNM-IMB, Nucl. Instrum. Meth. A592 (2008) 38–43.
[3] D. Sultan, et al., First Production of New Thin 3D Sensors for HL-LHC at FBK, JINST 12 (01) (2017) C01022.
[4] G. Kramberger, et al., Timing performance of small cell 3D silicon detectors`\path{arXiv:1901.02538}`.
[5] G. Kramberger, KDetSim: a simple way to simulate detectors, http://kdetsim.org.
[6] de La Taille, et al., ALTIROC0, a 20 pico-second time resolution ASIC for the ATLAS High Granularity Timing Detector (HGTD), PoS TWEPP-17 (2018) 006.